

### **Mechanics of Advanced Composite Structures**

Journal homepage: <a href="https://macs.semnan.ac.ir/">https://macs.semnan.ac.ir/</a>

ISSN: 2423-7043



#### Research Article

### Mechanical and Tribological Characterization of Eco-friendly Brake Pads using Banana Peel Powder as a Sustainable Friction Material

Javed Sikandar Shaikh all, Uday Aswalekar all, Amit Malgol b\*

- <sup>a</sup> Department of Mechanical Eng<mark>ineering, Vidyav</mark>ardhini's College of Engineering and Technology, Vasai, Palgar, 401202, Maharashtra, India.
  - b Department of Mechanical Engineering, "Agnel Charities", Fr. C. Rodrigues Institute of Technology, Vashi, Navi Mumbai, 400703, Maharashtra, India.

### ARTICLE INFO

### **ABSTRACT**

#### Article history:

Received: 2024-11-07 Revised: 2025-01-10 Accepted: 2025-10-02

#### Keywords:

Banana peel powder; Tribological properties; Coefficient of Friction; Asbestos; Wear rate; In this study, a novel brake pad material is developed from banana peel powder, offering a sustainable alternative for automotive friction applications. Banana peel powder with particle sizes of 100  $\mu m$ , 150  $\mu m$ , 300  $\mu m$ , and 400  $\mu m$  are utilized to fabricate the brake pads, with comprehensive characterization such as morphological, mechanical, physical, and tribological properties. Scanning Electron Microscopy is employed to investigate the uniform distribution and interfacial bonding of materials within the brake pad material. Brake pads incorporating banana peel powder of different particle sizes are evaluated to optimize oil resistance, water resistance, hardness, compressive strength, bulk density, and coefficient of friction. SEM analysis demonstrated a uniform distribution of BP powder sizes, ensuring strong interfacial bonding with the resin. The developed banana peel powder brake pads are evaluated on the front wheel of test vehicles under both smooth and hard braking conditions on highways and unpaved roads. Reducing BP size from  $400 \,\mu m$  to  $150 \,\mu m$  significantly enhanced oil and water resistance, hardness, compressive strength, and bulk density, while further reduction to 100  $\mu m$  offered marginal improvements. Consequently, a BP powder size of 150  $\mu m$  was identified as optimal. The average coefficient of friction (COF) for all BP pads (0.41-0.44) was comparable to commercial asbestos-based brake pads. The developed banana peel brake pads demonstrated wear rate, hardness, and coefficient of friction characteristics that are compared with commercial asbestos-based brake pads, demonstrating potential for eco-friendly brake pad applications.

© 2025 The Author(s). Mechanics of Advanced Composite Structures published by Semnan University Press. This is an open access article under the CC-BY 4.0 license. (https://creativecommons.org/licenses/by/4.0/)

### 1. Introduction

The braking system is a crucial mechanical component in vehicles and industrial machinery,

E-mail address: amitmalgol123@gmail.com

#### Cite this article as:

<sup>\*</sup> Corresponding author.

attributed to safely converting kinetic energy into heat through friction. The process not only decelerates or stops the motion of the system but also plays a crucial role in maintaining operational safety, stability, and control across diverse conditions. Asbestos has been widely used in brake pads since the early 20th century due to its excellent heat resistance and adaptability for blending into composite materials, making it the most employed material in brake pad manufacturing. Its structure enables easy weaving and integration with both organic and inorganic components. However, there is a critical demand to develop asbestos-free brake pad materials due to the carcinogenic properties of asbestos [1].

An ideal brake pad material must exhibit versatile mechanical and tribological properties, including high thermal stability, low wear rate, minimal noise under both smooth and hard braking, a stable coefficient of friction (COF), and environmental sustainability. However, due to the health hazards posed by asbestos's carcinogenic qualities, the Environmental Protection Agency (EPA) prohibited its usage. Although copper, a semi-metallic FM, has attracted significant attention over the last two decades, developed countries have begun to set limitations on its usage, and copper as an FM is anticipated to be prohibited by 2025 [1]. A critical need exists in the global industrial sector to find alternatives to FMs, which play a vital role in braking systems. With notable advancements in materials science, recent studies have explored the potential use of metallic, semi-metallic, lowmetallic, and composite materials as substitutes for traditional FM. The complex composition of FMs, typically involving over 15 constituents such as fibers, fillers, and binders [2].

Kalel et al. [2] fabricated eco-friendly brake pads using Aramid fibers/pulp and Zylon fibers to estimate the coefficient of friction. Aigbodion [3] investigated the performance of brake pads modified with silver nanoparticle-coated carbon nanotubes derived from rice husks. The results show that under optimal conditions, the wear rate and COF were 2.15 mg/m and 0.42, respectively. In some of the literature, asbestosfree brake pads were developed using cashew friction dust [1], silicon [4], bagasse ash [5], fine brass fibers [6], and periwinkle shell [7-8]. Chandradass et al. [9] investigated the tribological and mechanical properties of carbon fiber brake pads. The results showed that increasing the volume percentage of carbon resulted in increased COF, tensile and flexural strength, and a decreased wear rate. Sagiroglu and Akdogan [10]examined polymer-based brake pads utilizing blast furnace slag and observed that adding 50% slag improved the

coefficient of friction. Kiehl et al. [11] investigated the tribological performance of the gray cast iron brake pad coated with Stellite™ 6. The findings show that the Stellite<sup>TM</sup> 6 coating improved corrosion resistance by forming a passive layer of cobalt and chromium oxide. Carlevaris et al. [12] investigated the performance of FM based on rice husk and rice husk ash for the reduction of particulate material emissions and wear rate. Tej [13] evaluated the tribological properties of brake pads developed using cement bypass dust as a filler material, combined with barium sulfate. The results indicated that the COF initially increased with a rise in the weight percentage of cement bypass dust, and then further decreased with increased weight percentage. Bhakuni et al. [14] developed FM using ceramic matrix composites with kaolin clay and barite powder to evaluate the effect of wear resistance and COF. Zheng *et al.* [15] conducted a study on the friction and wear characteristics of FMs with added iron and graphite powders. Findings indicate that optimal frictional properties were achieved with iron and graphite mass contents of 20% and 14%, respectively. Xu et al. [16] performed a tribological analysis of copper-matrix FMs incorporating mullite and kvanite. Their findings revealed that kyanite contributed to the formation of a tribofilm on the surface of the FM, providing wear protection. Specifically, the addition of 1% kyanite reduced wear by approximately 30%. Selvam et al. [17] investigated the wear characteristics of brake pads developed from titanium alloy-based FMs, employing a titanium aluminum nitride coating to enhance the tribological properties of the pads. Jensen et al. [18] developed a wear model to analyze tribological behavior in brake pads, which they subsequently validated using data from a test vehicle equipped with brake pads. The evaluation included both smooth and hard braking on highway and unpaved roads, with varied braking frequencies. Their findings revealed significant disparities in wear patterns across the brake pads under both hard and smooth braking conditions.

An approach to developing sustainable FMs for braking systems involves the use of natural, eco-friendly resources. The existing literature reveals that various laboratory-synthesized FMs were employed in the development of asbestosfree and copper-free brake pads. However, a critical limitation of advanced synthetic FMs is the potential risk posed by organic and inorganic constituents to both human health and the environment. Moreover, existing literature primarily examines the performance of brake pads in laboratory settings, with limited experimental studies evaluating the performance of developed brake pads in test vehicles.

The current study proposes a novel FM for disc brakes derived from BP fibers, aiming to enhance environmental sustainability in brake component manufacturing. The brake pads were developed from BP powders of various sizes  $(100-400 \, \mu m)$  and tested for morphology and tribological properties. Further, optimized brake pads were physically tested on the front wheel of the test vehicle for hard and smooth braking over about 220 km, with frequent and infrequent braking on highways and unpaved roads.

The rest of the paper is organized as follows. In Section 2, the fabrication and characterization of the brake pads are performed, followed by results and discussions in Section 3. Finally, conclusions are drawn from the current study, and potential directions for future research are proposed in Section 4.

### 2. Material and Characterization

In this section, a detailed fabrication process and characterization techniques applied to brake pads are developed using BP powder.

### 2.1. Details Fabrication of Banana Peel (BP) Brake Pads

Bananas were sourced from local markets and subsequently cleansed in a fruit-washing machine for 20 minutes to effectively eliminate pesticide residues and surface contaminants. To facilitate the removal of the peels, bananas are immersed in hot water at a temperature range of 60-65 °C for a duration of 2-3 minutes, followed by a cooling period, and the peels are manually separated. The collected peels are segmented into halves or quarters and subsequently dried using an electric dryer set to 65°C for a duration of 20 minutes. The dehydrated BP's pulverized into fine and coarse powder. The samples were subsequently separated using a vibrating mesh screen, which ensured uniform particle size of  $100 \, \mu m$ ,  $150 \, \mu m$ ,  $300 \, \mu m$ , and  $400 \, \mu m$  for subsequent analyses. The sieving process was conducted using ASTM standard mesh sizes, ensuring precise classification of the powder into the desired particle size ranges. Figure 1 presents images illustrating various particle sizes of the prepared BP powders.



**Fig. 1.** Images of BP powder (a) 400  $\mu m$ , (b) 300  $\mu m$ , (c) 150  $\mu m$ , and (d) 100  $\mu m$ .

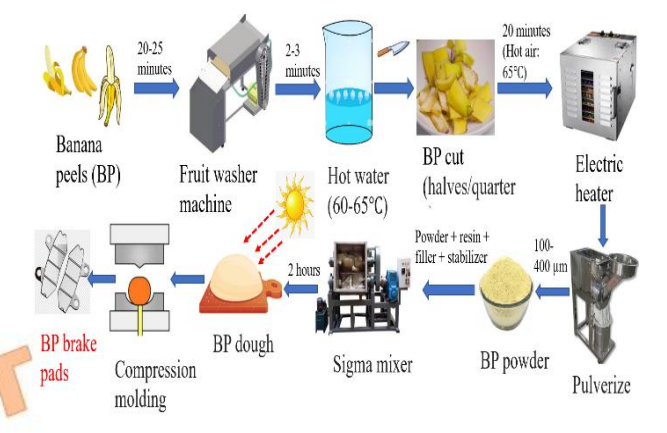


**Fig. 2.** Fabrication process of brake pads using banana peel powder

Brake pads are fabricated using BP powder various particle sizes through a compression molding process. The phenolic resin, along with non-metallic filler materials (mica and barium sulfate) and a stabilizer (cashew nutshell powder), is combined and mixed thoroughly in a sigma mixer for a duration of 25–30 minutes. The phenolic resin used as the binding agent is known for its excellent thermal stability, which allows it to withstand temperatures up to 300°C-350°C before decomposition [21-22]. Mica was selected for its excellent thermal stability and ability to enhance the wear resistance of the composite material. Barium sulfate, on the other hand, was employed to improve density and thermal conductivity. The uniformly mixed, viscous dough resulting from the preparation process is allowed to air-dry under direct sunlight for a period of 2 hours. The dried brake pads are fabricated using powdered BPs with various particle sizes through a compression molding process.





Fig. 3. (a) Test Vehicle (b) Sample brake pads

The phenolic resin, along with filler materials (mica and barium sulfate) and a stabilizer (cashew nutshell powder), is combined and mixed thoroughly in a sigma mixer for a duration of 25–30 minutes. The uniformly mixed, viscous dough resulting from the preparation process is allowed to air-dry under direct sunlight for a period of 2 hours. The dried dough is subsequently subjected to compression molding at a pressure of  $100\ bar$  and a temperature of  $140\ ^{\circ}$ C. Figure 2 illustrates the fabrication process for BP brake pads. Figure 3(a) and (b) show the test vehicle and brake pad sample, respectively.

### 2.2.Characterization of Banana Peel Brake Pads

The characterization of brake pads incorporating BP material was conducted to examine their morphological, mechanical, physical, and tribological properties. The morphology of the fabricated pad samples was analyzed using a scanning electron microscope (SEM, model SU6600, Hitachi, Japan). Prior to scanning electron microscopy (SEM) imaging, the pads are coated with a thin layer of gold sputter deposition to mitigate the accumulation of excess electrons. The prepared pads are immersed in SAE 80 engine oil (as per JIS D 4418) and water for a duration of 24 hours at a temperature range of  $27-30^{\circ}C$  to evaluate the oil and water absorption resistance of BP brake pads. The changes in weight and dimensions of the brake pads before and after immersion in water and engine oil were analyzed to investigate swelling. The bulk density was determined using

Archimedes' principle. The pads were immersed in water, and the volume of water displaced  $(V_w)$  was determined using the equation. (1), which relates the weight of the object in water  $(W_w)$  to the weight of the object in air  $(W_a)$ . Subsequently, the density  $(\rho)$  of the pad was calculated using eqn. (2).

The volume of water displaced (V<sub>w</sub>) is written

as,

$$V_{w} = \frac{W_{a} - W_{w}}{g\rho_{w}} \tag{1}$$

The density of the brake pad is calculated as,

$$\rho = \frac{\rho_{\rm w} W_{\rm a}}{W_{\rm a} - W_{\rm w}} \tag{2}$$

where g and  $\rho_w$  are the acceleration due to gravity and the density of water, respectively.

The hardness of the developed banana peel brake pads is assessed using the Brinell hardness tester. The pads were subjected to a load range of 981 to 1471 N for a duration of 15 seconds, utilizing a steel indenter with a diameter of 1.56 mm and a hardness value of approximately 101 BHN. The Brinell hardness number is determined using standardized charts and empirical formulas. Further, compression tests are conducted using an 11-Avery-Denison compression machine with a capacity of 2000 kN, at a strain rate of 0.0014 s<sup>-1</sup>. The brake pads are held in the testing machine and subjected to gradual loading until failure occurs.

The wear tests on the developed pads are performed using a pin-on-disc tribometer to evaluate two-body sliding wear in accordance with ASTM G 99-95a standards. The banana brake pads with a diameter of 10 mm, were subjected to contact with a rotating cast iron disc at a linear speed of  $1.5 \, m/s$  for a duration of 60 minutes under a load ranging from 30 to 50 N, without the application of lubrication. A cast iron disc, characterized by a hardness of 160 BHN, was employed, featuring a track diameter of 130 mm and a thickness of 10 mm. All experiments are conducted in a controlled environment maintained at a temperature range of 25 to 28 °C. The initial and final weight differences of the pad sample are measured using a precision balance with an accuracy of 0.0002 grams. The brake pad samples subjected to testing were thoroughly cleaned with acetone to eliminate surface contaminants. The wear rate  $(W_r)$  is calculated using the weight loss  $(W_s)$  in the sample and the sliding distance (S) as follows:

$$W_r = \frac{W_S}{S} \tag{3}$$

In the upcoming section, all the relevant and important results are discussed.

### 3. Results and Discussion

In this section, surface morphology, water and oil absorption, hardness, compressive strength, bulk modulus, wear rate, and COF are evaluated.

### 3.1. Effect of Particle Size on Surface Morphology

Figure 4 presents the morphology of BP brake pads with particle sizes of  $100 \, \mu m$ ,  $150 \, \mu m$ ,  $300 \, \mu m$ , and  $400 \, \mu m$ . The SEM images indicate that BP brake pads with various sizes exhibit a uniform elemental distribution and good interfacial bonding with the resin. The sigma mixer facilitated thorough powder blending, enhancing the uniform distribution of elemental components.

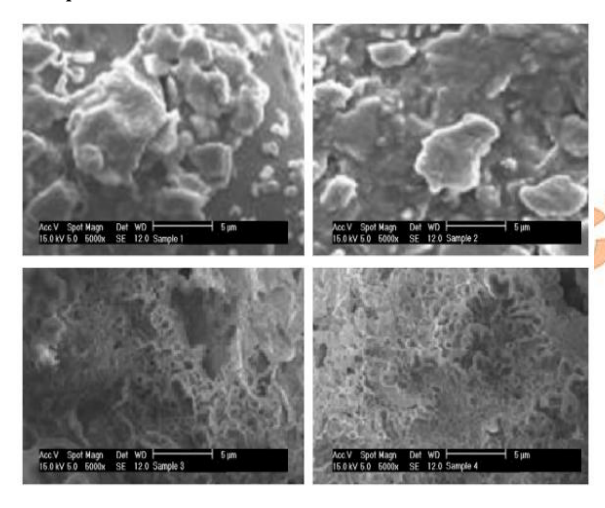


**Fig. 4.** SEM images of BP brake pads (a) Sample 1:  $400 \mu m$ , (b) Sample 2:  $300 \mu m$ , (c) Sample 3:  $150 \mu m$ , and (d) Sample 4:  $100 \mu m$ .

A detailed evaluation of SEM images (Fig. 4(a) -4(d)) indicates that powders with particle sizes of  $100~\mu m$  and  $150~\mu m$  shows a more consistent elemental distribution relative to other particle sizes. The effect of a reduction in powder particle size, which increases the specific surface area and subsequently enhances interfacial bonding with the resin.

# 3.2. Effect of Particle Size on Water and Oil Absorption

The absorption of oil and water by brake pads significantly reduces braking efficiency. The oil and water absorption properties of the pad surface are measured and analyzed to select an effective brake pad. Figure 5 illustrates the

thickness swelling of BP pads with various powdered sizes in water and engine oil (SAE 20W-50). The reduction in the BP powder particle size from  $400~\mu m$  to  $150~\mu m$  resulted in a significant decrease in the oil and water thickness-swelling properties. This phenomenon is attributed to enhanced elemental bonding resulting from a reduction in particle size, which consequently leads to decreased porosity.

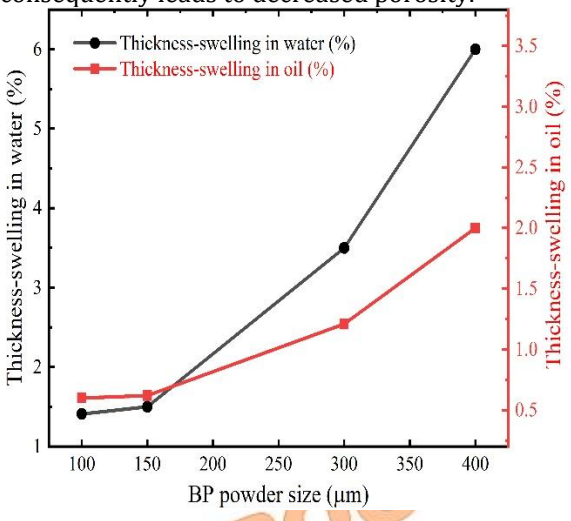


**Fig. 5.** Thickness swelling of BP brake pads with different powdered sizes in water and engine oil.

The reduction of peel powder particle size to  $100~\mu m$  resulted in a marginal decrease in the properties of the material. Therefore, a particle size of  $150~\mu m$  for the BP powder brake pad is considered optimal for minimizing oil and water absorption. The swelling of BP brake pads during immersion in water and engine oil is attributed to the compression stresses generated during compression modeling, as well as the hygroscopic properties of the material. It is noteworthy that the brake pads developed in this study demonstrated minimal swelling during water and engine oil absorption tests.

## 3.3. Effect of Particle Size on Hardness and Compressive Strength

A vital property influencing the selection of brake pads is hardness, a complex characteristic influenced by various mechanical properties, including compressive and tensile strengths, wear resistance, stiffness, and toughness. Figure 6 illustrates the impact of BP brake pad powder size on both hardness and compressive strength. The hardness value significantly increased as the peel powder size decreased from 400  $\mu m$  to 150  $\mu m$ . However, a further reduction in powder size to 100  $\mu m$  resulted in only a marginal increase in hardness. The reduction in powder size enhances the specific surface area, facilitating stronger bonding with the resin and

thereby increasing the hardness value. As shown in Fig. 6, the BP brake pad sample with a powder size of  $150~\mu m$  exhibited the highest hardness.

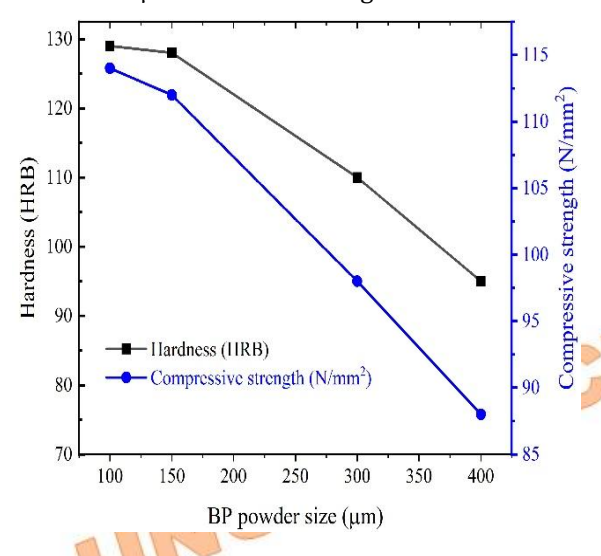


**Fig. 6.** Influence of BP powder size on the hardness and compressive strength of the brake pads.

Compressive strength demonstrates a similar trend to that of hardness, as it varies linearly with average hardness. The pads containing  $150~\mu m$  peel powder displayed reduced porosity, homogeneous elemental distribution, and improved interfacial bonding, resulting in the highest compressive strength.

### 3.4. Effect of Particle Size on Bulk Density

The density of brake pads is a critical factor influencing their lifespan and durability, as brake pads with higher density can effectively dissipate the heat generated during braking. Table 1 presents the estimated average density values for various brake pad samples. The average density exhibited a slight variation of approximately 1.2% in relation to powder size. This marginal decrease in bulk density with increasing powder particle size is attributed to a greater proportion of coarser particles, which diminishes interfacial bonding and, consequently, results in lower bulk density.

 Table 1. Bulk density of different BP brake pads.

BP pad with powder size	Bulk density
(µm)	(g/cm <sup>3</sup> )
400	1.68
300	1.67
150	1.66
100	1.66

# 3.5. Effect of Particle Size on Wear Rate $(W_r)$ and Coefficient of Friction (COF)

The brake pads with a high COF and a low wear rate can achieve effective braking. Figure 7 illustrates the variation in wear rate (W<sub>r</sub>) with load for various brake pad (BP) samples. These pad samples were tested at a constant sliding velocity of 1.5 m/s for 60 minutes. The wear rate (W<sub>r</sub>) and COF in the pin-on-disc tribometer are influenced by sliding velocity, distance, and load. In the current wear tests, BP pads are subjected to loads ranging from 30 N to 50 N. The results indicate that increasing the load raised the wear rate across all BP pad samples; this finding is consistent with observations made by Sivaprakasam et al. [19] in their wear study of titanium alloys.

The increased load generates greater pressure on the pad, allowing a hard, rough disc surface to cause more substantial material removal from the softer pad surface, thereby leading to increased mass loss and a higher wear rate. Although the abrasive mechanism is primarily responsible for surface wear, a small portion of wear may also be attributed to an adhesive mechanism, as the two surfaces slide against each other under dry conditions. This sliding generates intramolecular forces that facilitate the removal of fragments from the pad surfaces by the harder disc surfaces. The continuous increase in load enhances these intramolecular forces between the pad and disc surfaces, thereby elevating the contribution of the adhesive wear mechanism to the overall wear process.

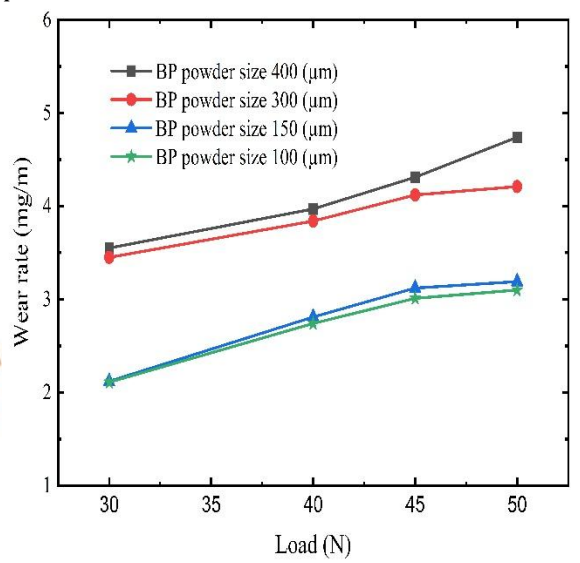


Figure 7 illustrates the variation in wear rates among the different BP pad samples. The BP pad features a powder size of  $400 \, \mu m$  exhibited substantial wear, whereas the pad with a powdered size of  $100 \, \mu m$  demonstrated minimal

wear. This difference is attributed to the reduced powdered size, which increases the specific surface area and enhances interfacial bonding with the resin, resulting in improved hardness (as shown in Fig. 6) and a subsequently lower wear rate. The BP pad with a powder size of 150  $\mu m$  was identified as optimal, as the wear rate exhibited only marginal variation when the powdered size was reduced to 100 um. The average COF for the various BP pads is summarized in Table 2. The COF of commercial asbestos-based brake pads ranges from 0.3 to 0.49 (ISO 6312:2010). The average COF for all BP pads falls within the range of commercial asbestos-based brake pads, as shown in Table 2. Notably, the highest average COF was observed for pads with powdered sizes of 150 µm and 100 μm, while the lowest was recorded for the pad with a powder size of 400  $\mu m$ .

Table 2. Average COF for different BP brake pads

1700	
BP pad with powder	COF
size (μm)	
400	0.41
300	0.42
150	0.44
100	0.44

The results demonstrated that the BP brake pads maintained a stable coefficient of friction (COF) within the range of 0.41 to 0.44, ensuring reliable stopping performance. The phenolic resin, which serves as the binding matrix, provides excellent thermal stability up to  $300^{\circ}\text{C}-350^{\circ}\text{C}$ , enabling the brake pads to withstand the rapid heat buildup associated with sudden braking. Figure 8 presents the morphology of BP brake pads with particle sizes of  $100~\mu m$ ,  $150~\mu m$ ,  $300~\mu m$ , and  $400~\mu m$ .

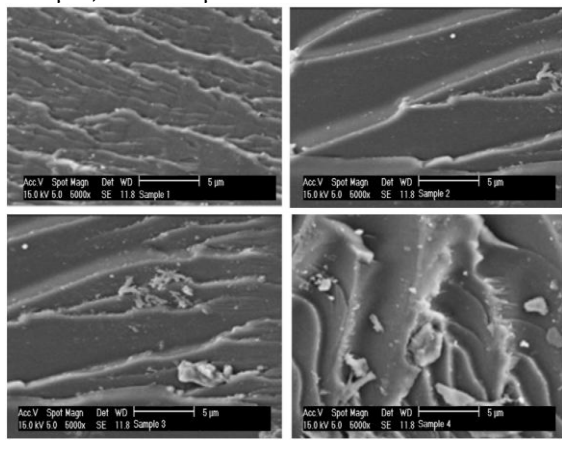


Fig. 8. Wear SEM images of BP brake pads (a) Sample 1: 100  $\mu m$ , (b) Sample 2: 150  $\mu m$ , (c) Sample 3: 300  $\mu m$ , and (d) Sample 4: 400  $\mu m$ .

### 3.6. Testing of the Developed BP Brake Pads on the Test Vehicle

The two BP pads with a particle size of 150 μm (BPP-150) are tested on the front wheel of the test vehicle. A medium-sized modern twowheeler is utilized as a test vehicle, which features a 4-stroke, 2-valve, single-spark gasoline engine and is equipped with disc brakes on both wheels. The BPPs-150 are installed exclusively on the left and right sides of the front wheel disc of the test vehicle. The wear performance of the developed BPP-150 is evaluated in a test vehicle under both smooth and hard braking conditions. In the smooth braking test, the vehicle maintained a relatively constant speed on the highway, with infrequent braking over long distances. In contrast, the hard braking test involved driving at a variable speed on a country or unpaved road, where purposeful braking occurred over short distances. The wear on the brake pads was assessed by removing them from the vehicle after every 20 km of travel, resulting total of 11 measurements approximately 220 km. Wear measurements are assessed at three distinct locations on the brake pad surface: the leading and trailing edges, and the center. Figure 9 illustrates the various wear measurement locations on both pad surfaces. Figures 10 and 11 depict the thickness variation of the left and right BPP-150 brake pads during both smooth and hard braking conditions. Wear was observed at all three measurement locations on the left and right pads under both braking conditions. Notably, the leading edges of both pads exhibited significant wear, followed by the trailing edges and centers. This uneven wear may be attributed to improper caliper operation. The guide pin of the caliper is designed to enable the brake pads to establish an equal contact angle with the disc; however, any malfunction of the guide pin leads to an unequal contact angle between the pads and the disc, resulting in uneven wear. In the present study, improper guide pin operation may cause the leading edge of the pads to make a greater contact angle with the disc, leading to increased wear. Moreover, a detailed examination of Figs. 10 and 11 indicate that both the left and right brake pad surfaces experienced greater wear during hard braking compared to smooth braking. This is primarily attributable to the frequent braking over short distances on unpaved roads. It is noteworthy that the wear on both BPP-150 pad surfaces is minimal, measuring approximately 0.1 mm, 0.08 mm, and 0.008 mm over the course of  $220 \, km$ .

The COF of BPP-150 brake pad prototypes (BPPs-150) was measured both before and after testing under vehicle conditions that included smooth and hard braking. The measurements are

conducted using a pin-on-disc tribometer, where the BPP-150 samples were machined into pin shapes ( $10 \ mm$  diameter) and mounted for testing. The vehicle's front wheel brake disc with a diameter of  $282 \ mm$  and a thickness of  $4 \ mm$ . The disc rotated at a speed of  $1.5 \ m/s$  for 60 minutes under a  $40 \ N$  load without lubrication, with all tests performed at temperatures between  $26-29^{\circ}C$ .

Figure 11 displays the average COF variation of BPP-150 pads on both the left and right sides during hard and smooth braking. The wear incurred led to a reduction in the average COF for both braking conditions, as shown in Figures 10 and 11. The COF of the developed brake pads remained within the SAE J866 standard range [18] after testing. The durability and friction characteristics of the BPP-150 pads were evaluated over an approximate distance of 220 km. Further long-distance testing, including both smooth and hard braking scenarios, is required to confirm their long-term viability.

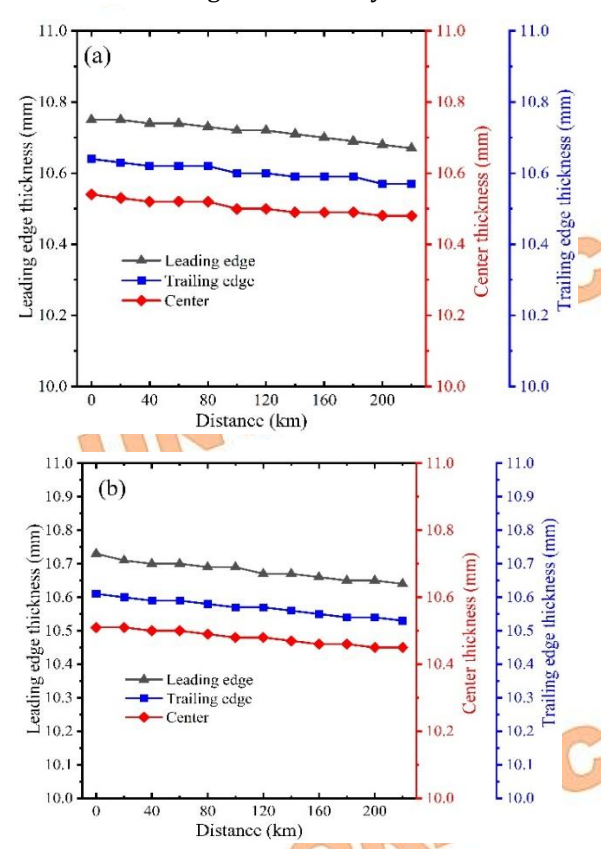


**Fig. 9.** Variation of the thickness of BPP-150 (a) left and (b) right side during smooth braking.

To evaluate the viability of the developed BP brake pad samples, Table 3 presents a comparative analysis of their properties against commercially available asbestos-based and asbestos-free brake pads reported in recent literature. Notably, the wear rate  $(W_r)$ , COF, and hardness values for the developed pads (with a particle size of  $150 \,\mu m$ ) comply with ISO 6312:2010 standards. However, the developed pads exhibit slightly higher swelling in oil and water, suggesting the need for additional antiswelling agents in their fabrication. Based on these findings, BP brake pads are recommended as potential replacements for commonly used asbestos-based pads. The approximate weight of vehicle is 135 kgs.

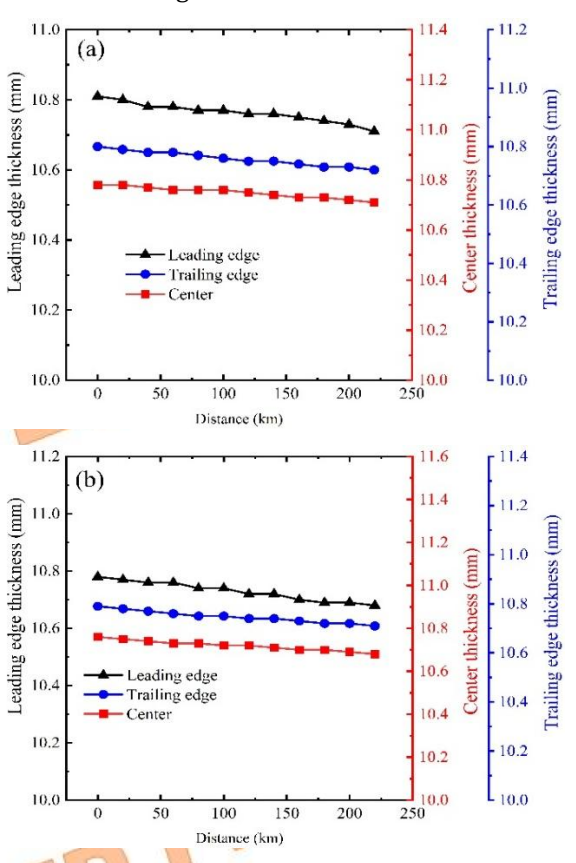


Fig. 10. Variation of the thickness of BPP-150 (a) left and (b) right side during hard braking.

In this study, noise levels produced by the developed banana peel (BP) powder brake pads were qualitatively assessed during testing under both smooth and hard braking conditions on highways and unpaved roads.

**Table 3.** Characteristic comparison of the developed BP brake pad (powder size  $150 \mu m$ ) with other brake pads.

Table of characteristic comparison of the developed B1 brake pad (powder size 100 km) with other brake pads.					
Characteristics	Hardness	Thickness-swelling in water (%)	Thickness-swelling in engine oil (%)	$W_r$	COF
	(BHN)	( )	0 ()	(mg/m)	
Asbestos-based commercial brake pads (ISO 6312:2010)	101	0.9	0.3	3.80	0.3 - 0.49

Banana fiber phenolic resin [21]	89 RHN	-	-	-	0.3-0.45
Bagasse material-based	100.5	3.48	1.11	4.20	0.42
pad [20] Rise husk material-	125	0.95	0.28	2.15	0.42
based pad [3] Current study	128	1.5	0.62	2.12	0.44 - 0.46

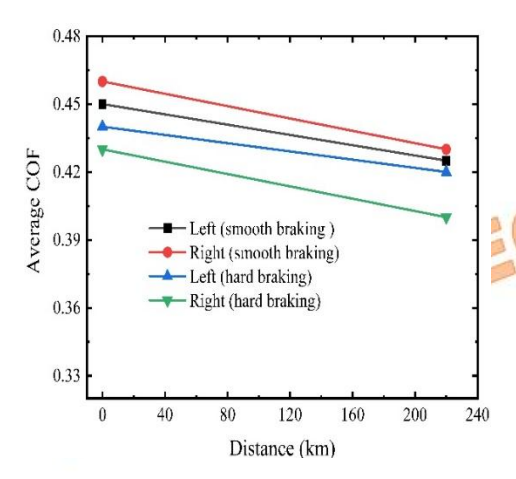


**Fig. 11.** Variation of the average COF of BPP-150 on the left and right sides during hard and smooth braking.

The noise generated during braking was found to be minimal, comparable to that of commercial asbestos-based brake pads. This can be attributed to the effective damping properties of the BP powder composite, which helps to absorb vibrations and reduce squealing.

### 4. Conclusions

The significant health hazards posed by asbestos-based brake pads; this study explored the use of BPs as an alternative material for fabricating asbestos-free brake pads. The brake pads are fabricated using BP powders of varying particle sizes  $(100\text{-}400\,\mu\text{m})$  and characterized for their morphological, mechanical, physical, and tribological properties. The performance testing was conducted on a test vehicle under both smooth and hard braking conditions. Key conclusions from the study are as follows:

- 1. Scanning electron microscopy (SEM) imaging revealed a consistent distribution of B powder particles in various size ranges (100  $\mu m$ , 150  $\mu m$ , 300  $\mu m$ , and 400  $\mu m$ ) within the material. This uniformity in particle size and dispersion suggests effective integration and dispersion of the BP powder throughout the resin matrix. Furthermore, the SEM analysis highlights strong interfacial bonding between the BP particles and the resin, which is critical for enhancing the material's mechanical properties and ensuring structural stability in applications.
- 2. The reduction of powder particle size from 400  $\mu m$  to 150  $\mu m$  significantly improved key

material properties, including oil and water resistance, hardness, compressive strength, and bulk density. This enhancement indicates that finer particles contribute to a more robust matrix, likely due to increased surface area facilitating better interparticle bonding and filling efficiency. In contrast, further size reduction to  $100\,\mu m$  yielded only marginal gains, suggesting that a particle size of  $150\,\mu m$  represents an optimal balance between mechanical performance and manufacturability.

- 3. The observed increase in wear mass loss during pin-on-disc tribometry as a function of applied load can be attributed to the elevated contact pressure, which enhances the abrasive interaction between the disc and the pad. This intensified contact not only promotes greater material displacement from the softer pad but also leads to more pronounced wear mechanisms, such as plowing and adhesion, due to the roughness and hardness of the disc surface exacerbating the degradation of the pad material.
- 4. The average coefficient of friction (COF) for BP pads was observed to range from 0.41 to 0.44, indicating a performance level that is competitive with that of traditional asbestos-based pads, which have long been recognized for their reliable frictional characteristics. This comparable COF suggests that BP pads may serve as a viable alternative in applications where effective friction management is crucial, while also aligning with contemporary sustainability goals by reducing reliance on asbestos materials.
- 5. During vehicle testing, a pronounced degree of wear was noted on the leading edges of the brake pads, indicating a potential correlation with the initial impact forces during braking. This was subsequently followed by wear patterns on the trailing edges and central regions, suggesting a comprehensive analysis of brake dynamics may be necessary to optimize performance and longevity.

These findings support the potential of BP-based brake pads as a viable, safer alternative to asbestos-based brake pads, with comparable tribological performance and enhanced environmental safety.

### **Nomenclature**

g Gravitational acceleration  $(m/s^2)$ 

S	Sliding	distance	(m)
---	---------	----------	-----

$V_{w}$	Volume of water displaced (	$(m^3)$	١
V <sub>W</sub>	volulile of water displaced	(111)	,

 $W_a$  Weight in air (kg)

 $W_r$  Wear rate (mg/m)

 $W_s$  Weight loss of brake pad (kg)

 $W_w$  Weight in water (kg)

ρ Density of brakepad  $(kg/m^3)$ 

 $\rho_{\rm w}$  Density of water  $(kg/m^3)$ 

BP Banana peel

BPP-150 Banana peel pads with a powder

size of 150 um

COF Coefficient of friction

FM Friction material

### **Acknowledgments**

The authors express our sincere gratitude to the Department of Mechanical Engineering, Vidyavardhini's College of Engineering and Technology, Vasai, Palgar, for providing the necessary facilities and support throughout this work.

### **Funding Statement**

This research did not receive any specific grant from funding agencies in the public, commercial, or not-for-profit sectors.

#### **Conflicts of Interest**

The author declares that there is no conflict of interest regarding the publication of this article.

### References

[1] Singaravelu, D.L., Vijay, R. and Filip, P., 2019. Influence of various cashew friction dusts on the fade and recovery characteristics of non-asbestos copper-free brake friction composites. *Wear*, 426–427, pp.1129–1141.

Doi: 10.1016/j.wear.2018.12.036

[2] Kalel, N., Bhatt, B., Darpe, A. and Bijwe, J., 2022. Exploration of Zylon fibers with various aspect ratios to enhance the performance of ecofriendly brake-pads. *Tribology International*, 167, p.107385. Doi: 10.1016/j.triboint.2021.107385

[3] Aigbodion, S.V., 2024. Unveiling the frictional properties of brake pads developed from silver nanoparticle-modified carbon nanotubes derived

from rice husks. *Tribology International*. Doi: 10.1016/j.triboint.2024.109270

[4] Manoj, E., Marshall, R.A., Muthupandi, K., Natarajan, R.B., Jacob, A., Jino, L., Jayaganthan, A. and Suthan, S.A., 2023. Investigation on the mechanical and tribological properties of silicon in an automotive brake pad. *Materials Today: Proceedings*, pp.1–5.

Doi: 10.1016/j.matpr.2023.01.129

[5] Chandradass, J., Surabhi, M.A., Sethupathi, P.B. and Jawahar, P., 2020. Development of low cost brake pad material using asbestos free sugarcane bagasse ash hybrid composites. *Materials Today: Proceedings*, 45, pp. 7050–7057.

Doi: 10.1016/j.matpr.2021.01.877

[6] Hendre, K. and Bachchhav, B., 2020. Tribological behaviour of non-asbestos brake pad material. *Materials Today: Proceedings*, 38, pp.2549–2554.

Doi: 10.1016/j.matpr.2020.07.560

[7] Yawas, D.S., Aku, S.Y. and Amaren, S.G., 2016. Morphology and properties of periwinkle shell asbestos-free brake pad. *Journal of King Saud University – Engineering Sciences*, 28, pp.103–109. Doi: 10.1016/j.jksues.2013.11.002

[8] Amaren, S.G., Yawas, D.S. and Aku, S.Y., 2013. Effect of periwinkle shell particle size on the wear behavior of asbestos free brake pad. *Results in Physics*, 3, pp.109–114.

Doi: 10.1016/j.rinp.2013.06.004

[9] Chandradass, J., Sethupathi, P.B. and Surabi, M.A., 2020. Fabrication and characterization of asbestos free epoxy based brake pads using carbon fiber as reinforcement. *Materials Today: Proceedings*, 45, pp.7222–7227.

Doi: 10.1016/j.matpr.2021.02.530

[10] Sagiroglu, S. and Akdogan, K., 2023. The effect of the addition of blast furnace slag on the wear behavior of heavy transport polymer-based brake pads. *Tribology International*, 189, p.108845. Doi: 10.1016/j.triboint.2023.108845

[11] Kiehl, M., Scheid, A., Graf, K., Ernst, B. and Tetzlaff, U., 2023. Coaxial laser cladding of cobaltbase alloy StelliteTM 6 on gray cast iron: investigations on friction. wear versus commercial brake pad, and corrosion characteristics. Proceedings of the Institution of Mechanical Engineers, Part D: Journal of Automobile Engineering, 14, pp.3285–3303. Doi: 10.1177/09544070221145512

[12] Carlevaris, D., Leonardi, M., Straffelini, G. and Gialanella, S., 2023. Design of a friction material for brake pads based on rice husk and its

derivatives. *Wear*, 526–527, p.204893. Doi: 10.1016/j.wear.2023.204893

[13] Singh, T., 2023. Comparative performance of barium sulphate and cement by-pass dust on tribological properties of automotive brake friction composites. *Alexandria Engineering Journal*, 72, pp.339–349.

Doi: 10.1016/j.aej.2023.04.010

[14] Bhakuni, H., Muley, A.V. and Ruchika, 2023. Fabrication, testing and analysis of particulate ceramic matrix composite for automotive brake pad application. *Materials Today: Proceedings*, pp.2214–2219.

Doi: 10.1016/j.matpr.2023.01.413

[15] Zheng, D., Zhao, X., An, K., Chen, L., Zhao, Y., Khan, D.F., Qu, X. and Yin, H., 2023. Effects of Fe and graphite on friction and wear properties of brake friction materials for high-speed and heavy-duty vehicles. *Tribology International*, 178, p.108061. Doi: 10.1016/j.triboint.2022.108061

[16] Xu, Z., Zhong, M., Xu, W., Xie, G. and Hu, H., 2023. Effects of aluminosilicate particles on tribological performance and friction mechanism of Cu-matrix pads for high-speed trains. *Tribology International*, 177, p.107983.

Doi: 10.1016/j.triboint.2022.107983

[17] Selvam, P.T., Pugazhenthi, R., Dhanasekaran, C., Chandrasekaran, M. and Sivaganesan, S., 2020. Experimental investigation on the frictional wear behaviour of TiAlN coated brake pads. *Materials Today: Proceedings*, 37, pp.2419–2426. Doi: 10.1016/j.matpr.2020.08.272

[18] Jensen, K.M., Santos, I.F. and Corstens, H.J.P., 2023. Estimation of brake pad wear and remaining useful life from fused sensor system, statistical data processing, and passenger car longitudinal dynamics. *Wear*, 538–539, p.205220. Doi: 10.1016/j.wear.2023.205220

[19] Sivaprakasam, P., Hailu, T. and Elias, G., 2023. Experimental investigation on wear behavior of titanium alloy (Grade 23) by pin on disc tribometer. *Results in Materials*, 19, p.100422. Doi: 10.1016/j.rinma.2023.100422

[20] Aigbodion, V.S., Akadike, U., Hassan, S.B., Asuke, S.B. and Agunsoye, J.O., 2010. Development of asbestos-free brake pad using bagasse. *Tribology in Industry*, 32, pp.12–18.

[21] Bashir, M., Qayoum, A. and Saleem, S.S., 2021. Experimental investigation of thermal and tribological characteristics of brake pad developed from eco-friendly materials. *Journal of Bio- and Tribo-Corrosion*, 7(66).

Doi: 10.1007/s40735-021-00502-x

[22] Ghosh, P., Banerjee, S.S. and Khastgir, D., 2020. Performance assessment of hybrid fibrous fillers on the tribological and thermo-mechanical behaviors of elastomer modified phenolic resin friction composite. *SN Applied Sciences*, 2, pp.1–14.

